

# Buoyant Mixing Processes Generated in Turbulent Plume Arrays

Pilar LÓPEZ GONZÁLEZ-NIETO<sup>1</sup>, José L. CANO<sup>1</sup> and José Manuel REDONDO<sup>2</sup>

<sup>1</sup> Universidad Complutense de Madrid. Departamento de Astrofísica y Ciencias de la Atmósfera.  
maplopez@bio.ucm.es, jlcano@fis.ucm.es

<sup>2</sup> Universidad Politécnica de Cataluña. Departamento de Física Aplicada.  
redondo@fa.upc.es

(Received 31 January 2007; received in revised form 21 June 2007; accepted 22 June 2007)

## ABSTRACT:

Turbulent mixing is a very important issue in the study of geophysical phenomena because most fluxes arising in geophysics fluids are turbulent. The diffusion of physical quantities in nature is due to turbulence. This is a key factor in the study of atmospheric phenomena, specially at the planetary boundary layer.

We study turbulent mixing due to convection using a laboratory experimental model with two miscible fluids of different density with an initial top heavy density distribution. Mixing is produced by the evolution of a two-dimensional array of forced turbulent plumes. Measurements include density data and flow visualization. The conclusions of this experimental model relate the mixing efficiency and the volume of the final mixed layer to the Atwood number, ranging from 0.010 to 0.134. We find that the number of plumes diminishes, the mixing efficiency reduces. We performed additional experiments releasing a fixed volume with negative buoyancy in a lighter fluid as a line of plumes (from one to nine) with a fixed Atwood number of 0.03, measuring the height of the final mixed layer as functions of the number of plumes and the available mixing volume.

**Key words:** atmospheric turbulence, turbulent mixing, unstable density distributions, turbulent plumes.

## Procesos de Mezcla Generados por un Conjunto de Penachos Turbulentos

### RESUMEN:

La mezcla turbulenta es un tema importante en el estudio de los fenómenos geofísicos porque los flujos geofísicos presentan flujos que son turbulentos en su gran mayoría. En la naturaleza, la difusión de las magnitudes físicas se realiza, principalmente, por medio de la turbulencia que, por tanto, es un factor clave en el estudio de los fenómenos atmosféricos, especialmente en la capa límite planetaria. En este artículo se estudia la mezcla turbulenta generada por un proceso de convección. Se utiliza un modelo experimental con dos fluidos miscibles de diferente densidad que inicialmente tiene una distribución inestable de densidad. La mezcla se genera por la evolución de un conjunto bidimensional de penachos turbulentos forzados. Las medidas incluyen datos de densidad y digitalizaciones del flujo. Las conclusiones hacen referencia a la eficiencia de mezcla y al volumen de la carga mezclada final relacionados con el número de Atwood, cuyos valores varían en el intervalo (0.010, 0.0134). Se encuentra que si el número de penachos disminuye, la eficiencia de mezcla decrece. Un mejor análisis de esta conclusión se hace mediante la realización de nuevos experimentos caracterizados por utilizar un conjunto lineal de penachos (desde uno hasta nueve) con los que se pone en contacto un volumen fluido fijo y con flotabilidad negativa con un fluido más ligero, siendo el número de Atwood 0.03. El objetivo de estos nuevos experimentos es medir la altura de la capa mezclada final en función del número de penachos y del volumen fluido disponible para la mezcla.

**Palabras clave:** turbulencia atmosférica, mezcla turbulenta, penachos turbulentos, eficiencia de mezcla, distribuciones inestables de densidad.

## 1. INTRODUCTION

Micrometeorology is the study of small-scale phenomena such as atmospheric turbulence with space scales smaller than about 3 km and with time scales shorter than about 1 h, which are classified as microscale. The study of the atmospheric boundary layer involves the study of microscale processes.

We focus our interests on analysing the turbulent mixed regime because of the important implications that this regime has to geophysical studies. The greatest part of the flows within geophysical fluid dynamics are turbulent—the atmospheric boundary layer, cumulus clouds or ocean currents—. In many phenomena occurring in nature, diffusion of physical quantities is governed by mixing generated by turbulence. This is specially important in the planetary boundary layer.

The definition and knowledge of atmospheric turbulence are essential due to the control it exerts upon the whole atmosphere as the diffusion. To investigate atmospheric turbulence, a deep understanding of the mixing processes is first required. Most pollutants sources, except aeroplanes, are close to the earth's surface. Pollutants are transported by turbulent atmospheric structures and, therefore, the inability of these structures to penetrate very far could trap pollutants. This happens if there is a stable stratification at the lower atmosphere which decreases the diffusion of pollutants because then the turbulence and the turbulent mixing decrease (Yagüe, 1992).

Additional motivations have come from the assumption that subsynoptic-scale phenomena, such as turbulence, might be responsible, in part, for the difficulty in making quality weather forecasts. Atmospheric turbulence is also important for other applications such agricultural meteorology or wind-generated power.

Buoyancy seems the dominant mechanism driving turbulence in a convective boundary layer. Such kind of turbulence is often organized into structures such as thermals and plumes. In the unstable surface layer there are small-scale structures such as buoyant vertical plumes, and higher in the mixed layer we observe larger-diameter thermals (Stull, 1988). All these structures are generated by heating at the bottom of the atmospheric boundary layer.

Plumes are coherent vertical structures of warm rising air with diameters and depths on the order of 100 m. Even though buoyancy is the dominant driven mechanism, the ambient mean wind modifies the plume structure. Wind shear causes the plumes to tilt, but plumes are more vertical when the shear is weak and the buoyancy strong (Stull, 1988).

Small-scale phenomena are transient in nature so a deterministic description and forecasting are virtually impossible. Micrometeorology has always relied heavily on field experiments, but they have relatively large costs. Alternative studies have used numerical and laboratory simulations. Much of the turbulence investigations has been performed in laboratory tanks. Although there have been many successful laboratory studies of small-scale turbulence, few experimental simulations of larger phenomena, such as thermals and plumes, have been made.

The difficulties of the direct investigation *in situ* of turbulent diffusion processes, such as those occurring in the lower atmosphere, force us to use substitute methods such as laboratory techniques and experimental models to

simulate natural phenomena. In experimental studies of real cases, the hydrodynamic and convective similarities are used to relate the real-life phenomena and the experimental model. For example, the growth of cumulus clouds has usually been modelled as a rising plume or a thermal, in both numerical and experimental setups. The growth of a plume or a thermal is expected to depend both on the buoyancy flux which causes internal turbulence and the degree of external turbulence.

Plumes are by itself a basic hydrodynamic model in order to simulate natural phenomena. For example, plume modelling is used to study natural and stack ventilation. Experimentally, salt solutions represent sources of buoyancy which are convenient to use because of mass conservation. Therefore, heat sources are modelled as dense plumes using salt water. Another example is wind advected smoke plumes which are not like the buoyant vertical plumes of the surface layer mentioned before. For air pollution and diffusion, smoke plumes are quasi-horizontal plumes downwind of an emission source.

We have briefly described how important is turbulent mixing and its implications to atmospheric phenomena. Thereafter we use a laboratory model to study turbulent mixing.

In the following sections, we provide a description of the experimental setup and of the fluid flows generated experimentally, as well as the observed mixing process. We present some characteristics of the mixing process, such as the height of the mixed layer  $h_M$  and the mixing efficiency  $\eta$ , based on measurements of the vertical profiles of density and the height of the fluid layers. Finally, the conclusions of our investigation are presented.

## **2. THE MIXING PROCESS**

Turbulent mixing is generated experimentally under an unstable density distribution in a fluid system. The fluids that form the initial unstable stratification are miscible and the turbulence will produce molecular mixing. The experiment described here is an unstable density distribution and, although it does not exactly correspond to a Rayleigh-Taylor case, one may still use similar experiments of the Rayleigh-Taylor instability as a guide (Sharp, 1984; Redondo & Linden, 1990, 1991; Linden et al., 1994).

The partial mixing process is characterized by the mixing efficiency and the volume of the final mixed layer as functions of the Atwood number,  $A = (\rho_D - \rho_L)/(\rho_D + \rho_L)$  with  $\rho_D$  the density of the top heavy fluid, which ranges from 0.010 to 0.134.

The unstable fluid system when released produces very active turbulent mixing which is initially forced by a discrete number of turbulent plumes whose interaction contributes to the mixing. Our aim is the study of the final properties of the mixed fluid after the turbulent mixing process.

There are many different procedures to obtain experimentally unstable density stratifications (Linden & Redondo, 1991; Linden et al., 1994; Ratafia, 1973; Read, 1984). Our experiment consists of three homogeneous fluids with different densities that are initially at rest. The complete description of the experiments

may be found at López, 2004. The fluids are placed inside a cubic glass container. At the bottom of the container, it is the fluid with lower density  $\rho_L$  and with a height  $h_L$ . On top of this light fluid layer, a sodiumcarboximethyl cellulose gel stratum, or CMC gel (American Society for Testing and Materials, 1989), is placed with density  $\rho_G$  and depth of  $h_G$ . The CMC gel is a non-newtonian time-dependent fluid and presents thixotropic behaviour. The presence of the CMC gel in the laboratory model slightly delays the mixing process to observe it better as well as generating a random initial structure. Finally, the fluid of greater density  $\rho_D$  (brine), which constitutes the *dense layer*, reaches a height  $h_D$  and is coloured with sodium fluorescent at low concentration which acts as a passive tracer (López, 2004).

The experiment begins with the dense fluid flow forming jets and they come into the gel layer. Therefore, the denser fluid impinges on the CMC gel layer, breaks down its surface tension and goes through the gel locally. The high gel viscosity (from 16000 cps to 44000 cps) and the small width of the gel layer make that the dense fluid flows in the laminar regime. There is no mixing between the dense fluid and the CMC gel. Finally, the dense fluid comes into the light fluid layer. The result is the generation of several forced plumes which are gravitationally unstable. The development of these plumes makes the turbulent mixing process possible (López, 2004).

The behaviour of this fluid system is influenced by the CMC gel viscosity  $\nu_G$ , the ratio of fluid densities, or Atwood number, and specially by the number of plumes  $n_p$  related to the initial conditions. As the turbulent plumes develop, the dense fluid comes into contact with the light fluid layer and the mixing process between them evolves as an array of turbulent plumes (López, 2004).

The final result of the mixing process is a heavier mixed layer located at the bottom of the experimental container: This mixed layer is separated from the non-mixed light fluid by a stable and quite sharp density interface. Since not all of the lighter fluid participates in the mixing, we qualify it as a partial mixing process. On the other hand, the final mixed layer obtained experimentally is not homogeneous, but has a stable density stratification.

Summing up, initially, we have an array of axisymmetric turbulent plumes which develop at an intermediate stage. This development is caused by the lateral interaction between these plumes at the complex fractal surface between the dense and light fluids. As the turbulence decays, a stable situation with internal waves takes place.

This behaviour of the mixing process is clearly shown in Fig. 1(a)-(i) which represents a frame sequence corresponding to the time evolution of a turbulent mixing process directly visualized and digitized (Dalziel, 2005). These frames show the development of a turbulent mixing process. The CMC gel density is  $\rho_{Gel} = 1.02 \text{ g/cm}^3$ , the gel viscosity is  $\mu_{Gel} = 16000 \text{ cps}$  and the Atwood number is  $A=0.019$  for this experiment.

Fig. 2(a) shows the start of a turbulent mixing process where the CMC gel used is more viscous one ( $\mu_{Gel}=44000 \text{ cps}$ ) and the Atwood number is  $A= 0.130$ . Fig. 2(b) shows another mixing process where the CMC gel used is less viscous

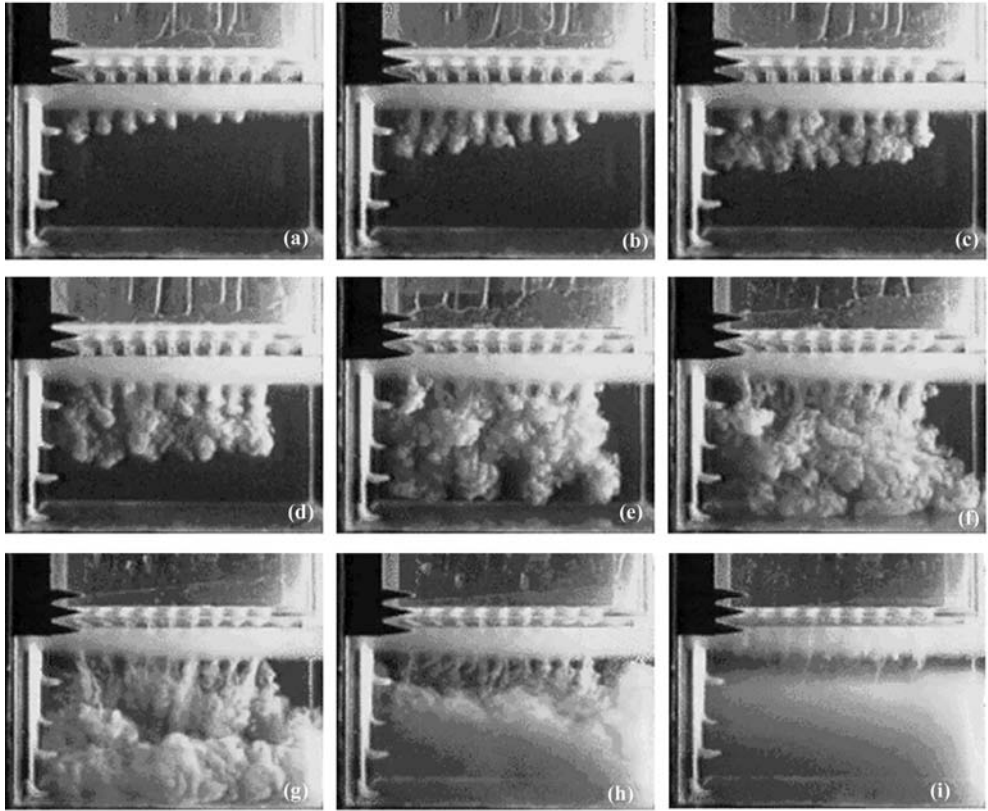


**Figure 1.-** Frame sequence of a experimental mixing process which experimental characteristics are:  $\rho_{Gel}=1.02 \text{ g/cm}^3$ ,  $\mu_{Gel}= 16000 \text{ cps}$  and  $A=0.019$ . (a) Start of the time evolution of the mixing process with several turbulent plumes which are clearly separated ( $t= 0.28 \text{ s}$ ). (b) Vertical development of the turbulent plumes. There is no protuberance in the CMC gel layer ( $t= 0.40 \text{ s}$ ). (c) The lateral interaction of turbulent plumes starts while they are growing ( $t= 0.56 \text{ s}$ ). (d) The lateral interaction between turbulent plumes is greater than in (c) ( $t= 0.80 \text{ s}$ ). (e) The mixing convective front evolves through the light fluid layer. General interaction between plumes ( $t= 1.44 \text{ s}$ ). (f) Non uniform evolution of the mixing convective front. The interaction of the fluid system with the contours of the container starts ( $t= 2.36 \text{ s}$ ). (g) A gravity current develops through the light fluid layer. This gravity current reaches the front of the experimental container ( $t= 4.76 \text{ s}$ ). (h) The mixing process fills the volume of the experimental container. Incipient formation of the mixed layer ( $t= 11.96 \text{ s}$ ). (i) Final state after the partial mixing process. We can observe the mixing layer limited by the stable density interface ( $t= 94 \text{ s}$ ).

( $\mu_{Gel}=16000 \text{ cps}$ ) and the Atwood number is  $A= 0.134$ . Both Atwood numbers are almost equal because we want to describe just the gel effect. If we compare these figures we observe clearly a lower number of turbulent plumes and the appearance of gel protuberances in Fig. 2(a) because the gel viscosity is greater than in Fig. 2(b). As the gel viscosity is reduced (from  $16000 \text{ cps}$  to  $44000 \text{ cps}$ ), the probability of initial generation of gel protuberances reduces, so that the formation of turbulent plumes increases as we see in Fig. 2(b) (López, 2004).



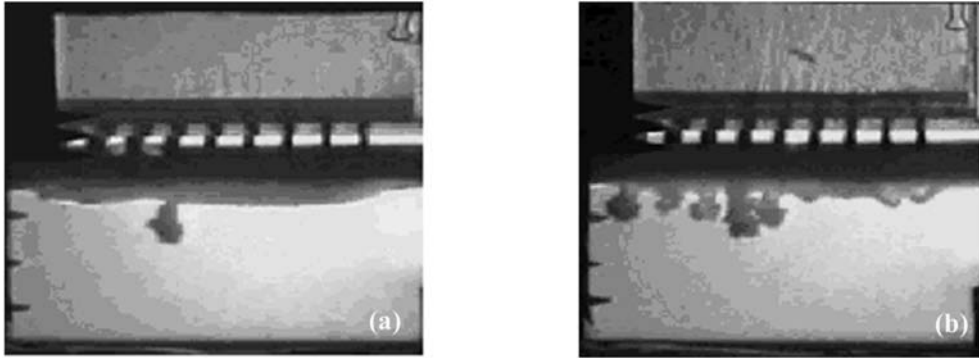


**Figure 2.-** (a) Partial mixing process with the most viscous CMC gel ( $\rho_{Gel}=1.03 \text{ g/cm}^3$  and  $\mu_{Gel}=44000 \text{ cps}$ ) and Atwood number of 0.130. The CMC gel layer is lightly deformed. A slight protuberance in the CMC gel can be seen together with an incipient turbulent plume which grows vertically ( $t=0.48 \text{ s}$ ). (b) Partial mixing process with the less viscous CMC gel ( $\rho_{Gel}=1.02 \text{ g/cm}^3$  and  $\mu_{Gel}=16000 \text{ cps}$ ) and Atwood number of 0.134. There are several turbulent plumes which are growing. There is no CMC gel protuberance ( $t=0.28 \text{ s}$ ).

The other factor having an effect on the fluid flow is the Atwood number  $A$  which represents the strength of the buoyancy effect. Comparing Figs. 3(a) and 3(b) we observe that the number of the turbulent plumes is greater in Fig. 3(a) than in Fig. 3(b) because the Atwood number is greater (from  $A=0.134$  to  $A=0.037$ ) while the gel viscosity is the same in both figures (López, 2004).

If the value of the Atwood number is greater, there is more available potential energy for the mixing process. This implies a greater quantity of mixed fluid, and therefore, a greater height of the mixed layer and of the mixing efficiency.

This effect of the Atwood number on the height of the mixed layer is shown in Figs. 4(a) and 4(b). Comparing these figures we observe that the height of the mixed

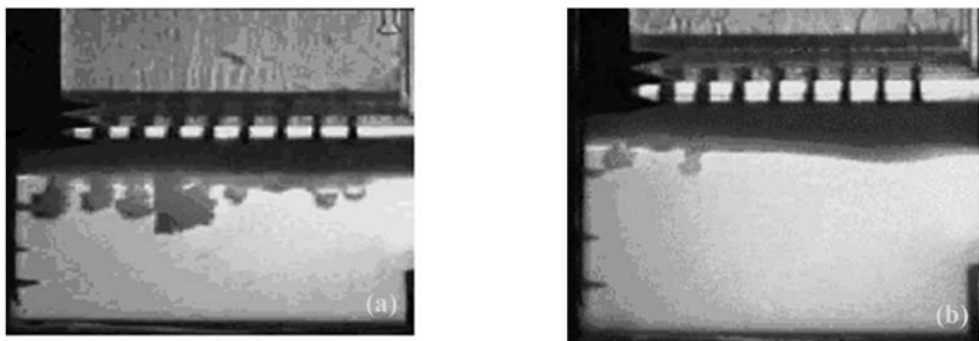


**Figure 3.-** Partial mixing process with the less viscous CMC gel ( $\rho_{Gel}=1.02 \text{ g/cm}^3$  and  $\mu_{Gel}=16000 \text{ cps}$ ). (a) Atwood number  $A=0.134$ . We can see the vertical development and the lateral interaction of turbulent plumes ( $t=0.32 \text{ s}$ ). (b) Atwood number  $A=0.037$ . We can see a slight protuberance in the CMC gel layer and the incipient formation of some turbulent plumes ( $t=0.32 \text{ s}$ ).

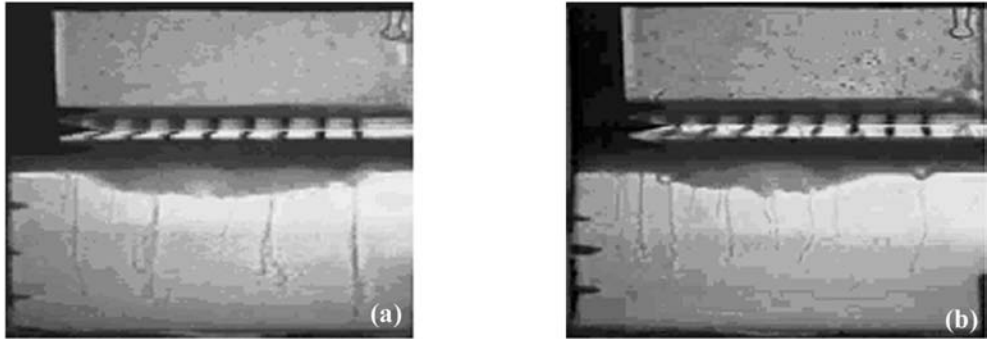


**Figure 4.-** Partial mixing process with the most viscous CMC gel ( $\rho_{Gel}=1.03 \text{ g/cm}^3$  and  $\mu_{Gel}= 44000 \text{ cps}$ ) (a) Atwood number of  $A=0.130$ . Final state of the partial mixing process. We can observe the mixing layer limited by the stable density interface ( $t= 95.16 \text{ s}$ ). (b) Atwood number of  $A=0.092$ . Final state of the partial mixing process. We can observe the mixing layer limited by the stable density interface ( $t= 81.52 \text{ s}$ ).

layer  $h_M$  is greater in Fig. 4(a) than in Fig. 4(b). The reason is the greater Atwood number which implies that the quantity of mixed fluid grows. This mixed fluid makes the mixed layer and, therefore, a greater height of the mixed layer appears.

### 3. RESULTS OF THE MIXING PROCESS

The behaviour of the experimental fluid system is governed by the turbulent energy source generated by the buoyancy. There are several factors that influences overall mixing. Specifically, it depends on three factors: The CMC gel used and its viscosity  $\nu_G$ . The Atwood number  $A$ , and the direct geometrical effect that the initial conditions have over the volume where mixing can take place (López, 2004).

The partial mixing process is characterized by two global properties: the mixing efficiency  $\eta$  and the mixed layer height  $h_M$  which both depend on the characteristics of the fluid system at the initial and final states. As the mixing process is influenced by the initial buoyancy, these two global properties are analyzed versus the Atwood number  $A$  which is proportional to the buoyancy. In addition, the mixing efficiency and the mixed layer height are also influenced by the presence of the CMC gel.

The final state of the fluid system is characterized by the presence of a stable density stratification. The mixed layer height  $h_M$  represents the final height of this stable density interface and it was measured experimentally. This height  $h_M$  is directly proportional to the final quantity, or volume, of the mixed fluid. The volume of the mixed fluid increases as the Atwood number grows and, consequently, the height of the mixed layer,  $h_M$ , is greater. In other words, as the buoyancy effect increases so does the convective turbulent mixing. This behaviour is shown in Fig. 5 which represents the non-dimensional mixed layer height  $h_M$  versus the Atwood number.

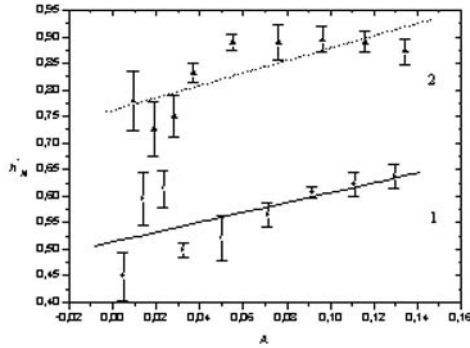


**Figure 5.-** Behaviour of the non-dimensional height of the mixed layer  $h_M^*$  with the Atwood number  $A$  for experiments made with the most viscous CMC gel, ( $\mu_{Gel}= 44000$  cps, Curve 1,  $\bullet$ ), and with the less viscous one ( $\mu_{Gel}= 16000$  cps, Curve 2,  $\blacktriangle$ ). The figure shows the linear fits done.

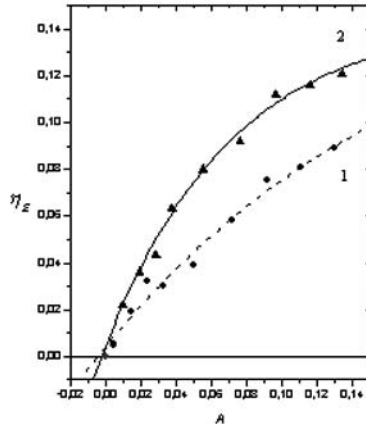


**Figure 6.-** Mean mixing efficiency  $\eta$  versus the Atwood number  $A$  for experiments made with the most viscous CMC gel ( $\mu_{Gel}= 44000$  cps, Curve 1,  $\bullet$ ), and with the less viscous one ( $\mu_{Gel}= 16000$  cps Curve 2,  $\blacktriangle$ ). The corresponding empirical fits are shown.

The effect of the gel viscosity may also be observed in the Fig. 5. The mixed layer height  $h_M$  increases if the gel used is the less viscous one ( $\mu_{Gel}=16000$  cps) because the number of turbulent plumes is greater when the gel viscosity is reduced (from 44000 cps to 16000 cps).

The denser and the lighter fluids do not mix completely which implies that the mixing process is only partial. The mixing efficiency  $\eta$  is analyzed, where  $\eta$  is defined as the fraction of the available energy used to mix fluids. The values of the mixing efficiency are obtained from the potential energy change that occurs during the mixing process. The definition of the mixing efficiency  $\eta$  is (Linden & Redondo, 1991; Linden et al., 1994; Redondo, 2001):



$$\eta = 1 - \frac{(\Delta Ep)_{PARTIAL}}{(\Delta Ep)_{NOMIX}} \quad (1)$$

where  $(\Delta Ep)_{PARTIAL}$  is the actual variation of potential energy associated to the partial mixing process.  $(\Delta Ep)_{NOMIX}$  is the potential energy change of a process without mixing (the denser fluid and the lighter one only exchange positions).

In Fig. 6 we plot the average mixing efficiency as a function of the Atwood number of the fluid system. In general, we observe that the efficiency increases as the Atwood number  $A$  does. Physically, the increase of the Atwood number implies that the buoyancy effect grows. Therefore, it produces a greater mixing process with a greater efficiency. Curve 2 of Fig. 6 shows that experiments done with the less viscous gel have a mixing efficiency greater if we compare them to experiments made with the most viscous gel shown in curve 1. The reason is the greater number of turbulent plumes created when the gel viscosity is reduced (from 44000 cps to 16000 cps).

In our experiment, we deduce that the final mixed layer is stratified. The observation of the final density profiles shows a strong density step, and, therefore we assume that the stratification of the mixed layer is made up by two layers. If the final profile is stratified, then the mixing efficiency is about 0.17 (Linden et al., 1992) and it has an upper limit of 0.18. Other scientific works state that the maximum mixing efficiency is reached when the final profile is totally mixed and homogeneous; this value is 0.5. Therefore, our efficiency is about 20% of the maximum mixing efficiency in comparable experiments.

In general, the mixing efficiency values are small if we compare them with the efficiency of a Rayleigh-Taylor instability –although the global evolution is right-. There are two reasons for these different values. First, the gel layer reduces efficiency about 40% if we compare it to experiments without gel (López, 2004). Second, the turbulent plume array generated during the evolution of the experiments (López et al., 2004).

We propose two hypotheses to understand these mixing efficiency differences and the effect of the plume array. Our first hypothesis is related to the dynamical behaviour of turbulent plumes: there is an interpenetration of the unstable plumes only through a fraction of the area at the top because once the dense fluid loses its potential energy it may not mix with the lighter fluid above. Therefore, the denser fluid and the lighter one do not mix completely which implies that a lower mixing efficiency is expected. Our second hypothesis is the effect of the greater number of plumes generated if the gel viscosity is reduced.

The experimental setup generates a two-dimensional plume array which makes conical volumes without mixing as Fig. 7 shows. This non-mixing volume makes a lower volume useful to mix because it is inside the light fluid layer. Therefore, the mixing efficiency must diminish. All turbulent plumes feed on the ambient light fluid. As a consequence there is a height  $h$  which represents the start of plume lateral interaction which determines the non-mixing volume. The start time of lateral interaction ranges from 1.042 s for a two plumes experiment to 0.336 s for a nine plumes experiment.

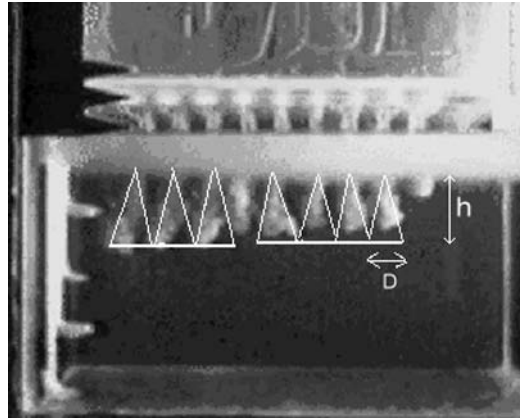


**Figure 7.-** Vertical development of the turbulent plumes with a superimposed scheme which represents their initial growth. Every plume is represented by a cone which radius is the plume radius,  $R$ . The lateral interaction between plumes starts at a depth  $h$ . The height of the light fluid layer is  $h_L$ . Experimental characteristics:  $\rho_{Gel}=1.02 \text{ g/cm}^3$ ,  $\mu_{Gel}= 16000 \text{ cps}$  and  $A=0.019$ .

A brief theoretical study allows us to deduce the non-mixing volume. We suppose that all turbulent plumes are approximated by cones. Their lateral interaction starts at a height  $h$  when they have a radius  $R$  and a diameter  $D$ . The total volume of the light fluid layer is approximated by the volume of a set of  $n$  cylinders concentric with  $n$  cones. These cylinders have radius  $R$  and diameter  $D$ . The mixing process occurs from the height  $h_L - h$  to the bottom of the experimental container, but not before. So, the useful volume where the mixing is possible has the following expression (López, 2004):

$$V_{USEFUL} = n\pi R^2 (h_L - h) \tag{2}$$

Then, we can deduce the expression of the non-mixing volume:

$$V_{NON-MIXING} = \frac{2}{3} n\pi R^2 h \tag{3}$$

which we make dimensionless dividing it by the total volume:

$$V_{NON-MIXING}^* = \frac{2h}{3h_L} \tag{4}$$

Therefore, the non-dimensional mixing volume has the expression:

$$V_{MIXING}^* = \left( 1 - \frac{2h}{3h_L} \right) \tag{5}$$

which represents the decrease of the mixing volume  $V_{MIXING}^*$  if the height ratios  $h/h_L$  increases because plumes reach a larger depth without interacting. The greater mixing volumes appear when plumes interact as soon as possible. We deduce that the non-dimensional mixing volume varies from 86% if the height ratios is  $(h/h_L)=1/5$  to 66% if  $(h/h_L)=1/2$ . The non-mixing volume  $V_{NON-MIXING}^*$  has the opposite behaviour which influences the mixing efficiency. This brief study demonstrates our first hypothesis: the dynamical behaviour of plumes reduces the mixing efficiency because they generate a smaller volume useful to mix.

The second hypothesis to understand our mixing efficiency values is that the mixing efficiency increases if the number of turbulent plumes is greater. To verify this hypothesis, we perform new experiments with a line of plumes –from one to nine plumes- with an Atwood number of 0.03. The new experiments are performed using different brine concentrations as the two mixing fluids. The experimental setup is the same described before (López, 2004), but we don't use the viscoelastic gel because we want to control the number of plumes and their geometric configuration into a line array.

We want to investigate better the relation between the non-mixing volume  $V_{NON-MIXING}^*$ , the number of plumes  $n_p$  and the mixing efficiency  $\eta$ . We also want to evaluate the results showed in Fig. 6, i.e., the lower the gel viscosity, the higher the mixing efficiency is. At this point, we must remember that if the gel viscosity is reduced, the number of plumes  $n_p$  increases. Therefore, it might exist a relation between the mixing efficiency and the number of plumes.

The mixing efficiency  $\eta$  is related to the mixing volume  $V_{MIXING}^*$ . Therefore it is also related to the inverse of the non-mixing volume  $V_{NON-MIXING}^*$  which can be represented by the non-mixing height,  $h_{NM}$ . For these reasons we measure the non-mixing height and we relate it to the number of plumes. We measure the number of plumes,  $n_p$ , and the non-mixing height directly from the digitalisations of the experiments. The new results are shown in Fig. 8.

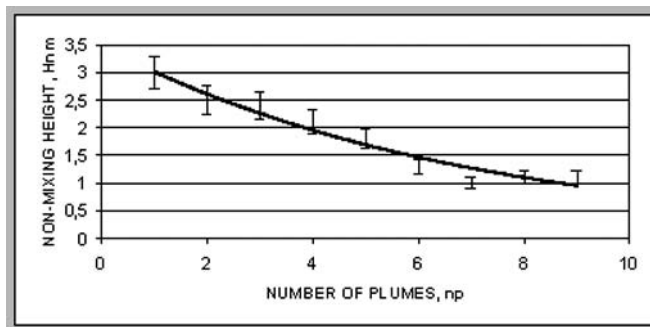


**Figure 8.-** Graphic behaviour of the non-mixing height,  $h_{NM}$ , versus the number of plumes,  $n_p$ . If the number of plumes,  $n_p$ , is greater, the non-mixing height decreases and, therefore, the non-mixing volume also decreases.

The Fig. 8 shows us that the greater the number of plumes,  $n_p$ , the less the non-mixing height is and the less the non-mixing volume is. Then the mixing efficiency is greater. This conclusion agrees with results deduced from Fig. 6. Therefore, we have verified that the initial conditions modify the overall mixing efficiency, i. e., the number of plumes affects the mixing efficiency.

#### 4. CONCLUSIONS

In many of the physical phenomena occurring in nature the diffusion of physical quantities is governed by the mixing generated by turbulence. To properly understand atmospheric and oceanic turbulence, for example, a deep understanding of the mixing processes is first required.

The paper investigates the turbulent mixing due to convection. The mixing process is generated by the evolution of a two-dimensional array of forced turbulent plumes. The global conclusions of this experiment are related to the mixing efficiency and the volume of the final mixed layer as functions of the Atwood number and gel viscosity.

The paper presents some important conclusions related to the global mixing efficiency behaviour for different initial conditions. We deduce that if the number of plumes decreases, the mixing efficiency also diminishes because the non-mixing height increases.

The structure of the plume array may be seen in the digitalisations of the experiments. The front growth in accordance with other authors and analyzed with DigiFlow is seen to depend strongly on initial conditions, i.e. the number and structure of the plume array.

#### REFERENCES

- AMERICAN SOCIETY FOR TESTING AND MATERIALS (1989). *Designation D1439: Standard Test Methods for Sodium Carboxymethylcellulose*.
- DALZIEL, S. (2005). *DigiFlow DL Research Partners DigiFlow Userguide Version 1.0*. Cambridge University Press.
- LINDEN, P. F. & J. M. REDONDO (1991). Molecular mixing in Rayleigh-Taylor instability. Part 1. Global mixing. *Phys. Fluids*, 5 (A), 1267-1274.
- LINDEN, P. F., J. M. REDONDO & C. P. CAULFIELD (1992). *Advances in Compressible Turbulent Mixing*. Edited by W.P. Dannevik, A.C. Buckingham & C.E. Leith, Princeton University.
- LINDEN, P.F., J. M. REDONDO & D. YOUNGS (1994). Molecular mixing in Rayleigh-Taylor Instability. *J. Fluid Mech*, 265, 97-124.
- LÓPEZ GONZÁLEZ-NIETO, P. (2004). *PhD Thesis*. Universidad Complutense de Madrid, Madrid, Spain.
- LÓPEZ GONZÁLEZ-NIETO, P., J. M. REDONDO, J. L. CANO & C. YAGÜE (2004). The role of inicial conditions on Rayleigh-Taylor mixing efficiency. *Internacional Workshop on the Physics of Compressible Turbulent Mixing*. Ed. Dalziel S., DAMTP, Cambridge University, U.K.

- RATAFIA, M. (1973). Experimental investigation of Rayleigh-Taylor instability. *Phys. Fluids* 16 (8), 1207-1210.
- READ, K. I. (1984). Experimental investigation of turbulent mixing by Rayleigh-Taylor instability. *Physica* 12D, 45-58.
- REDONDO, J. M. (2001). Mixing efficiency of different kinds of turbulent processes and instabilities. In: Linden, P. F. & J. M. Redondo (Eds.) *Turbulent mixing in Geophysical Flows*, CIMNE, Barcelona. 131-157.
- REDONDO J.M. & P.F. LINDEN (1990). Mixing produced by Rayleigh-Taylor instabilities. *Proceedings of Waves and Turbulence in stably stratified flows*. IMA Conference. Ed. S.D. Mobbs.
- SHARP, D. H. (1984). An overview of Rayleigh-Taylor Instability, *Physica* 12D, 3.
- STULL, R. B. (1988). *An introduction to boundary layer meteorology*. Kluwer Academic Publishers, Netherland, 666 pp.
- YAGÜE, C. (1992). *PhD Thesis*. Universidad Complutense de Madrid, Madrid. Spain.